Inorg. Chem. **2003**, *42*, 1163–1169

Multi-Iron Tungstodiarsenates. Synthesis, Characterization, and Electrocatalytic Studies of $\alpha\beta\beta\alpha$-$(Fe^{III}OH_2)_2Fe^{III}_2(As_2W_{15}O_{56})_2^{12-}$

Israel Martyr Mbomekalle,[†] Bineta Keita,[†] Louis Nadjo,*[,†] Patrick Berthet,[‡] Kenneth I. Hardcastle,[§] Craig L. Hill,*[,§] and Travis M. Anderson[§]

Laboratoire de Chimie Physique, UMR 8000, CNRS, Université Paris-Sud, Bâtiment 420, 91405 Orsay Cedex, France, Laboratoire de Physico Chimie de l'Etat Solide, UMR 8648, CNRS, Université Paris-Sud, Bâtiment 410, 91405 Orsay Cedex, France, and Department of Chemistry, Emory University, Atlanta, Georgia 30322

Received October 17, 2002

Reaction of the trivacant lacunary complex, α-$Na_{12}[As_2W_{15}O_{56}]$, with an aqueous solution of $Fe(NO_3)_3 \cdot 9H_2O$ yields the sandwich-type polyoxometalate, $\alpha\beta\beta\alpha$-$Na_{12}(Fe^{III}OH_2)_2Fe^{III}_2(As_2W_{15}O_{56})_2$ (Na**1**). The structure of this complex, determined by single-crystal X-ray crystallography (a = 13.434(1) Å, b = 13.763(1) Å, c = 22.999(2) Å, α = 90.246(2)°, β = 102.887(2)°, γ = 116.972(1)°, triclinic, $P\bar{1}$, R1 = 5.5%, based on 25342 independent reflections), consists of an Fe^{III}_4 unit sandwiched between two trivacant α-$As_2W_{15}O_{56}^{12-}$ moieties. UV–vis, infrared, cyclic voltammetry, and elemental analysis data are all consistent with the structure determined from X-ray analysis. Magnetization studies confirm that the four Fe(III) centers are antiferromagnetically coupled. A cyclic voltammogram of Na**1** reveals that a three-wave W(VI) system replaces the two-wave W(VI) system found in the precursor α-$As_2W_{15}O_{56}^{12-}$ complex. The observed modifications in the CV patterns of Na**1** and α-$As_2W_{15}O_{56}^{12-}$ are most likely due to subsequent changes in the acid–base properties of two reduced POMs that occur as a result of Fe(III) incorporation. Na**1** is shown to be more efficient than the monosubstituted complex α_2-$As_2(Fe^{III}OH_2)W_{17}O_{61}^{7-}$ in the electrocatalytic reduction of dioxygen. This is attributed to cooperativity effects among the adjacent Fe(III) centers in Na**1**.

Introduction

Polyoxometalates (POMs) are a large and rapidly growing class of metal−oxygen anionic clusters.[1−4] Current interest in polyoxometalate chemistry is driven by the diverse and highly alterable sizes, shapes, charge densities, acidities, and reversible redox potentials of these compounds. These properties have led to many applications in catalysis,[5−10] medicine,[11] and materials science.[12−14] We are presently seeking ways to promote simultaneous multielectron transfer reactions in POMs, which typically proceed by series of single-electron steps in the potential domain useful for electrocatalysis and where neither POM structure change nor electrode derivatization occurs.[15−22]

* Authors to whom correspondence should be addressed. E-mail: nadjo@lcp.u-psud.fr (L.N.); chill@emory.edu (C.L.H.).
[†] Laboratoire de Chimie Physique.
[‡] Laboratoire de Physico Chimie de l'Etat Solide.
[§] Emory University.

(1) Pope, M. T. *Heteropoly and Isopoly Oxometalates*; Springer-Verlag: Berlin, 1983.
(2) *Polyoxometalates: From Platonic Solids to Anti-retroviral Activity*; Pope, M. T.; Müller, A., Eds.; Kluwer Academic Publishers: Dordrecht, Netherlands, 1993.
(3) Topical issue on polyoxometalates: Hill, C. L., Guest Ed. *Chem. Rev.* **1998**, *98*, 1−389.
(4) *Polyoxometalate Chemistry: From Topology via Self-Assembly to Applications*; Pope, M. T., Müller, A., Eds.; Kluwer Academic Publishers: Dordrecht, Netherlands, 2001.
(5) Hill, C. L.; Prosser-McCartha, C. M. *Coord. Chem. Rev.* **1995**, *143*, 407−455.
(6) Okuhara, T.; Mizuno, N.; Misono, M. *Adv. Catal.* **1996**, *41*, 113−252.
(7) Mizuno, N.; Misono, M. *Chem. Rev.* **1998**, *98*, 199−218.
(8) Kozhevnikov, I. V. *Chem. Rev.* **1998**, *98*, 171−198.
(9) Neumann, R. *Prog. Inorg. Chem.* **1998**, *47*, 317−370.
(10) Katsoulis, D. E. *Chem. Rev.* **1998**, *98*, 359−388.
(11) Rhule, J. T.; Hill, C. L.; Judd, D. A.; Schinazi, R. F. *Chem. Rev.* **1998**, *98*, 327−357.
(12) Day, V. W.; Klemperer, W. G. *Science* **1985**, *228*, 533−541.
(13) Coronado, E.; Gómez-García, C. J. *Chem. Rev.* **1998**, *98*, 273−296.
(14) Müller, A.; Kogerler, P.; Kuhlmann, C. *Chem. Commun.* **1999**, 1347−1358.
(15) Keita, B.; Nadjo, L.; Contant, R.; Fournier, M.; Hervé, G. French Patent (CNRS) 89/1, 728, Feb 10, 1989.
(16) Keita, B.; Nadjo, L.; Contant, R.; Fournier, M.; Hervé, G. European Patent (CNRS), Appl. EP 382, 644, *Chem. Abstr.* 114: 191882 u.
(17) Keita, B.; Belhouari, A.; Nadjo, L.; Contant, R. *J. Electroanal. Chem.* **1995**, *181*, 243−250.
(18) Toth, J. E.; Anson, F. C. *J. Am. Chem. Soc.* **1989**, *111*, 2444−2451.
(19) Toth, J. E.; Anson, F. C. *J. Electroanal. Chem.* **1989**, *256*, 361−370.
(20) Keita, B.; Essaadi, K.; Nadjo, L.; Contant, R.; Justum, Y. *J. Electroanal. Chem.* **1996**, *404*, 271−279.

10.1021/ic0261169 CCC: $25.00
Published on Web 01/23/2003

Taking advantage of the continuous progress in the synthesis and characterization of POMs,[23−26] which has generated numerous families of compounds suitable for physicochemical studies, we recently identified three factors that promote multi-electron-transfer reactions in POMs.[27−35] First, the pH of the solution is important because it will determine, at least partly, the stability domain of the POM as well as the merging of waves by ECE-type mechanisms.[27] Second, a "substituent effect" was identified in which one or more of the skeletal d^0 (usually W^{VI} or Mo^{VI}) centers of the POM structure are replaced by d-electron-containing transition metal cations.[28−33] It was found that the location, nature, and number of the d-electron metals in the POM framework may influence the interactions between redox active centers within the molecule. Specifically, a comparison of the catalytic activity of $\alpha\beta\beta\alpha$-$(Cu^{II}OH_2)_2Cu^{II}_2(H_4AsW_{15}O_{56})_2^{18-}$ (based on the novel asymmetrical Wells−Dawson complex $H_4XW_{18}O_{62}^{7-}$, where X = P(V)[26] or As(V)[34]) with those of the analogous monosubstituted Cu−POMs demonstrated a favorable effect of the accumulation of copper centers in the electrocatalytic reduction of nitrate.[34] More recently, the nature of the central heteroatom was found to be a third factor in the promotion of multielectron redox reactions.[35] A comparison of a series of monosubstituted Wells−Dawson tungstodiphosphates and tungstodiarsenates revealed that the first several voltammetric waves are driven in a more positive potential (i.e., more favorable) direction by the presence of the As heteroatom.

These observations stimulated our interest in the sandwich-type polyoxometalates containing d-electron metal centers already known for their catalytic properties. Sandwich-type POMs are formed by the fusion of two trivacant POM moieties via a rhombus of four edge-sharing transition metal ions (Figure 1). Since the first Keggin-derived complexes (formula $TM_4(PW_9O_{34})_2$) were reported in 1973 (followed by the Wells−Dawson complexes of formula $TM_4(P_2W_{15}O_{56})_2$), the number of sandwich-type POMs has increased manyfold.[36−61]

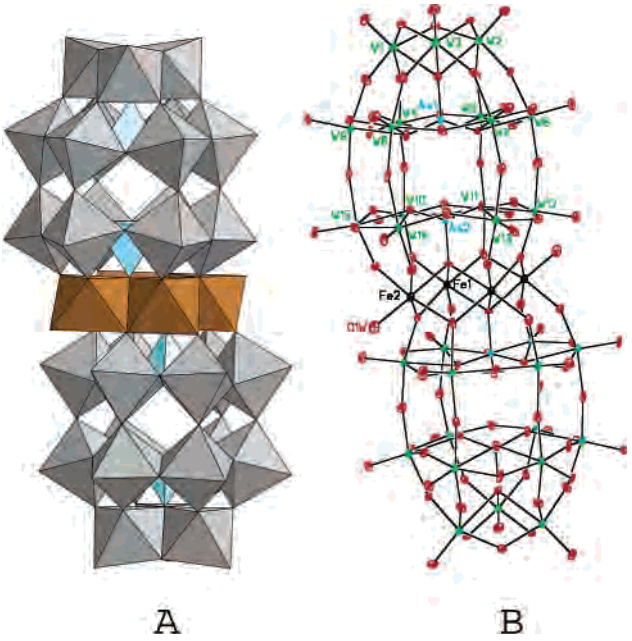

Figure 1. (A) Polyhedral representation of $\alpha\beta\beta\alpha$-$(Fe^{III}OH_2)_2Fe^{III}_2(As_2W_{15}O_{56})_2^{12-}$ (Na**1**). (B) Thermal ellipsoid plot (50% probability surfaces) of Na**1**.

(21) Keita, B.; Nadjo, L. *Mater. Chem. Phys.* **1989**, *22*, 77−103.
(22) Sadakane, A.; Steckhan, E. *Chem. Rev.* **1998**, *98*, 219−237.
(23) Contant, R. In *Inorganic Syntheses*; Ginsberg, A. P., Ed.; John Wiley and Sons: New York, 1990; Vol. 27, pp 104−111.
(24) Lyon, D. K.; Miller, W. K.; Novet, T.; Domaille, P. J.; Evitt, E.; Johnson, D. C.; Finke, R. G. *J. Am. Chem. Soc.* **1991**, *113*, 7209−7221.
(25) Baker, L. C. W.; Baker, V. E. S.; Eriks, K.; Pope, M. T.; Shibata, M.; Rollins, O. W.; Fang, J. H.; Koh, L. L. *J. Am. Chem. Soc.* **1966**, *88*, 2329−2331.
(26) Contant, R.; Spiro-Sellem, S.; Canny, J.; Thouvenot, R. *C. R. Acad. Sci., Ser. IIc: Chim.* **2000**, *3*, 157−161.
(27) Keita, B.; Nadjo, L. *Curr. Topics Electrochem.* **1993**, *2*, 77−106.
(28) Keita, B.; Lu, Y. W.; Nadjo, L.; Contant, R.; Abbessi, M.; Canny, J.; Richet, M. *J. Electroanal. Chem. Interfacial Electrochem.* **1999**, *477*, 146−157.
(29) Contant, R.; Abbessi, M.; Canny, J.; Richet, M.; Keita, B.; Belhouari, A.; Nadjo, L. *Eur. J. Inorg. Chem.* **2000**, 567−574.
(30) Contant, R.; Abbessi, M.; Canny, J.; Belhouari, A.; Keita, B.; Nadjo, L. *Inorg. Chem.* **1997**, *36*, 4961−4967.
(31) Keita, B.; Belhouari, A.; Nadjo, L.; Contant, R. *J. Electroanal. Chem.* **1998**, *442*, 49−57 and references therein.
(32) Keita, B.; Girard, F.; Nadjo, L.; Contant, R.; Canny, J.; Richet, M. *J. Electroanal. Chem.* **1999**, *478*, 76−82.
(33) Belghiche, R.; Contant, R.; Lu, Y. W.; Keita, B.; Abbessi, M.; Nadjo, L.; Mahuteau, J. *Eur. J. Inorg. Chem.* **2002**, 1410−1414.
(34) Keita, B.; Mbomekalle, I. M.; Nadjo, L.; Contant, R. *Electrochem. Commun.* **2001**, *3*, 267−273.
(35) Keita, B.; Mbomekalle, I. M.; Nadjo, L.; Contant, R. *Eur. J. Inorg. Chem.* **2002**, 473−479.
(36) Weakley, T. J. R.; Evans, H. T., Jr.; Showell, J. S.; Tourné, G. F.; Tourné, C. M. *J. Chem. Soc., Chem. Commun.* **1973**, *4*, 139−140.
(37) Finke, R. G.; Droege, M.; Hutchinson, J. R.; Gansow, O. *J. Am. Chem. Soc.* **1981**, *103*, 1587−1589.
(38) Finke, R. G.; Droege, M. W. *Inorg. Chem.* **1983**, *22*, 1006−1008.
(39) Evans, H. T.; Tourné, C. M.; Tourné, G. F.; Weakley, T. J. R. *J. Chem. Soc., Dalton Trans.* **1986**, 2699−2705.
(40) Wasfi, S. H.; Rheingold, A. L.; Kokoszka, G. F.; Goldstein, A. S. *Inorg. Chem.* **1987**, *26*, 2934−2939.
(41) Finke, R. G.; Droege, M. W.; Domaille, P. J. *Inorg. Chem.* **1987**, *26*, 6, 3886−3896.
(42) Tourné, C. M.; Tourné, G. F.; Zonnevijlle, F. *J. Chem. Soc., Dalton Trans.* **1991**, 143−155.
(43) Casañ-Pastor, N.; Bas-Serra, J.; Coronado, E.; Pourroy, G.; Baker, L. C. W. *J. Am. Chem. Soc.* **1992**, *114*, 10380−10383.
(44) Gómez-García, C. J.; Coronado, E.; Gómez-Romero, P.; Casañ-Pastor, N. *Inorg. Chem.* **1993**, *32*, 89−93.
(45) Gómez-García, C. J.; Coronado, E.; Gómez-Romero, P.; Casañ-Pastor, N. *Inorg. Chem.* **1993**, *32*, 3378−3381.
(46) Clemente, J. M.; Coronado, E.; Galán-Mascarós, J. R.; Gómez-García, C. J. *Inorg. Chem.* **1999**, *38*, 55−63.
(47) Zhang, X.-Y.; O'Connor, C. J.; Jameson, G. B.; Pope, M. T. *Inorg. Chem.* **1996**, *35*, 30−34.
(48) Weakley, T. J. R.; Finke, R. G. *Inorg. Chem.* **1990**, *29*, 1235−1241.
(49) Khenkin, A. M.; Hill, C. L. *Mendeleev Commun.* **1993**, 140−141.
(50) Gómez-García, C. J.; Borrás-Almenar, J. J.; Coronado, E.; Ouahab, L. *Inorg. Chem.* **1994**, *33*, 4016−4022.
(51) Finke, R. G.; Weakley, T. J. R. *J. Chem. Crystallogr.* **1994**, *24*, 123−128.
(52) Zhang, X.; Chen, Q.; Duncan, D. C.; Campana, C.; Hill, C. L. *Inorg. Chem.* **1997**, *36*, 4208−4215.
(53) Zhang, X.; Chen, Q.; Duncan, D. C.; Lachicotte, R. J.; Hill, C. L. *Inorg. Chem.* **1997**, *36*, 4381−4386.
(54) Rusu, M.; Marcu, G.; Rusu, D.; Rosu, C.; Tomsa, A.-R. *J. Radioanal. Nucl. Chem.* **1999**, *242*, 467−472.
(55) (a) Bi, L. H.; Wang, E.-B.; Peng, J.; Huang, R. D.; Xu, L.; Hu, C. W. *Inorg. Chem.* **2000**, *39*, 671−679. (b) Bi, L. H.; Huang, R. D.; Peng, J.; Wang, E.-B.; Wang, Y.-H.; Hu, C.-W. *J. Chem. Soc., Dalton Trans.* **2001**, 121−129.
(56) Kortz, U.; Isber, S.; Dickman, M. H.; Ravot, D. *Inorg. Chem.* **2000**, *39*, 2915−2922.
(57) Zhang, X.; Anderson, T. M.; Chen, Q.; Hill, C. L. *Inorg. Chem.* **2001**, *40*, 418−419.
(58) Anderson, T. M.; Hardcastle, K. I.; Okun, N.; Hill, C. L. *Inorg. Chem.* **2001**, *40*, 6418−6425.

We now report the synthesis and characterization of a new multi-iron sandwich-type POM, $\alpha\beta\beta\alpha$-$(Fe^{III}OH_2)_2Fe^{III}_2(As_2W_{15}O_{56})_2^{12-}$ (**1**). The phosphorus analogue of this compound ($\alpha\beta\beta\alpha$-$(Fe^{III}OH_2)_2Fe^{III}_2(P_2W_{15}O_{56})_2^{12-}$ (**2**)) was originally reported by Hill and co-workers.[52] The tetra-*n*-butylammonium salt of this complex was shown to be a modestly effective homogeneous catalyst for the H_2O_2-based epoxidation of alkenes. The title complex, **1**, is characterized by IR, UV−vis, elemental analysis, cyclic voltammetry, magnetization, and X-ray crystallography. Complex **1** is effective in the electrocatalytic reduction of dioxygen and hydrogen peroxide.

Experimental Section

General Methods and Materials. The starting sample of α-$K_6[As_2W_{18}O_{62}]\cdot 14H_2O$ was prepared according to our recently optimized method.[62] α-$Na_{12}[As_2W_{15}O_{56}]$ was obtained by published procedures, and purity was confirmed by IR and cyclic voltammetry.[55a] Elemental analyses of As, Fe, and Na were performed by CNRS Service Central d'Analyse at Vernaison (France). Quantitative analysis of W was performed in our laboratory by a modified literature method.[63] Infrared spectra (1% sample in KBr) were recorded on a Perkin-Elmer Spectrum One FT-IR instrument. The electronic absorption spectra were recorded on a Perkin-Elmer Lambda 19 spectrophotometer. Magnetic measurements were carried out on polycrystalline samples using a SQUID magnetometer, Quantum Design MPMS-5.

Synthesis of $\alpha\beta\beta\alpha$-$Na_{12}(FeOH_2)_2Fe_2(As_2W_{15}O_{56})_2\cdot 54H_2O$ (Na1). A 0.81 g (2 mmol) sample of $Fe(NO_3)_3\cdot 9H_2O$ was dissolved in 15 mL of deionized water, and 4.5 g (1 mmol) of solid α-$Na_{12}[As_2W_{15}O_{56}]$ was added slowly with vigorous stirring of the solution. The solution was heated at 60 °C until most of the liquid was evaporated (approximately 1 h), and the solution was filtered hot. The yellow precipitate that forms upon cooling is recrystallized from a minimal amount of 1 M NaCl. Yellow, diffraction-quality crystals were formed upon standing for several hours (yield 37%). IR (1% KBr pellet, 1300−400 cm^{-1}): 937 (s), 889 (sh), 866 (w), 820 (m), 796 (sh), and 744 (m). Anal. Calcd for $H_{112}As_4Fe_4O_{168}W_{30}$: As, 3.29; Fe, 2.45; Na, 3.03; W, 60.51. Found: As, 3.05; Fe, 2.31; Na, 3.26; W, 59.75. [MW = 9115.]

X-ray Crystallography. A suitable crystal of Na**1** was coated with Paratone N oil, suspended on a small fiber loop, and placed in a stream of cooled nitrogen (100 K) on a Bruker D8 SMART APEX CCD sealed tube diffractometer with graphite monochromated Mo Kα (0.71073 Å) radiation. A sphere of data was measured using combinations of ϕ and ω scans with 10 s frame exposures and 0.3° frame widths. Data collection, indexing, and initial cell refinements were carried out using SMART software (Version 5.624, Bruker AXS, Inc., Madison, WI). Frame integration and final cell refinements were carried out using SAINT software (Version 6.02, Bruker AXS, Inc., Madison, WI). The final cell parameters were determined from least-squares refinement. A multiple absorption correction for each data set was applied using the program SADABS (Version 2.03, George Sheldrick, University of Göttingen). The structure was solved using direct methods and difference Fourier techniques (SHELXTL, V5.10). All Fe, As, and W atoms were refined anisotropically. All oxygen atoms were also refined anisotropically except the following: O(10), O(33), O(47), O(53), O(15w), O(27w), O(28w), O(29w), and O(30w). Some of the solvent waters were disordered within the crystal lattice and were refined with partial occupancy (O(27w), 0.55; O(28w), 0.7; O(29w), 0.5; O(30w), 0.5). The final R1 scattering factors and anomalous dispersion corrections were taken from the *International Tables for X-ray Crystallography*.[64] Structure solution, refinement, graphics, and generation of publication materials were performed using SHELXTL, V5.10 software. Additional details are given in Table 1, and a thermal ellipsoid plot (at the 50% probability level) is given in Figure 1B. Disorder of the Na^+ countercations prevented the identification of all 12 Na atoms.

Table 1. Crystal Data and Structure Refinement for Na**1**

empirical formula	$As_4Fe_4Na_{11}O_{167.5}W_{30}$
fw	8971.47
cryst syst	triclinic
space group	$P\bar{1}$
unit cell	$a = 13.434(1)$ Å
	$b = 13.763(1)$ Å
	$c = 22.999(2)$ Å
	$\alpha = 90.246(2)°$
	$\beta = 102.887(2)°$
	$\gamma = 116.972(1)°$
V	3667.0(5) $Å^3$
Z	1
abs coeff	24.858 mm^{-1}
reflns collected	62284
indep reflns	25342
GOF on F^2	1.051
final R indices [$R > 2\sigma(I)$]	$R1^a = 0.0550$
	$wR2^b = 0.1481$

^{a} $R1 = \sum||F_o| - |F_c||/\sum|F_o|$. ^{b} $wR2 = \{\sum[w(F_o^2 - F_c^2)^2]/\sum[w(F_o^2)^2]\}^{0.5}$.

Electrochemical Experiments. A pH 5 buffer solution composed of 0.4 M CH_3COOLi and CH_3COOH was used for all experiments. Solutions were deaerated with Ar for 30 min before measurements and kept under a positive pressure at all times. All electrochemical measurements were performed with an EG and G 273A apparatus under computer control (M270 software). The source, mounting, and polishing of the glassy carbon electrodes (GC, Tokai, Japan) have been previously described.[65] The glassy carbon samples had a diameter of 3 mm. Potentials are quoted against a saturated calomel electrode (SCE). The counter electrode was a platinum gauze of large surface area. All experiments were performed at ambient temperature.

Results and Discussion

Synthesis and Characterization of Na1. The complex, Na**1**, was readily prepared in ∼30% yield and in high purity. Two slightly different procedures were used to obtain the complex. The first method was adapted from that described for the phosphorus analogue $\alpha\beta\beta\alpha$-$(Fe^{III}OH_2)_2Fe^{III}_2(P_2W_{15}O_{56})_2^{12-}$ (**2**).[52] A second procedure was developed which gave higher yields (37% yield versus 30% yield for the first method) and better quality crystals (suitable for X-ray

(59) (a) Ruhlmann, L.; Nadjo, L.; Canny J.; Contant, R.; Thouvenot, R. *Eur. J. Inorg. Chem.* **2002**, 975−986. (b) Ruhlmann, L.; Canny, J.; Contant, R.; Thouvenot, R. *Inorg. Chem.* **2002**, *41*, 3811−3819.
(60) Anderson, T. M.; Zhang, X.; Hardcastle, K. I.; Hill, C. L. *Inorg. Chem.* **2002**, *41*, 2477−2488.
(61) (a) Kortz, U.; Savelieff, M. G.; Bassil, B. M.; Keita, B.; Nadjo, L. *Inorg. Chem.* **2002**, *41*, 783−789. (b) Kortz, U.; Mbomekalle, I. M.; Keita, B.; Nadjo, L.; Berthet, P. *Inorg. Chem.* **2002**, *41*, 6412−6416.
(62) Mbomekalle, I. M.; Keita, B.; Nadjo, L.; Contant, R.; Belai, N.; Pope, M. T. *Inorg. Chim. Acta.* **2003**, *342*, 219−228.
(63) Lis, S.; But, S. *J. Alloys Compd.* **2000**, *303*−*304*, 132−136.
(64) *International Tables for X-ray Crystallography*; Kynoch Academic Publishers: Dordrecht, Netherlands, 1992; Vol. C.
(65) Keita, B.; Girard, F.; Nadjo, L.; Contant, R.; Belghiche, R.; Abbessi, M. *J. Electroanal. Chem.* **2001**, *508*, 70−80.

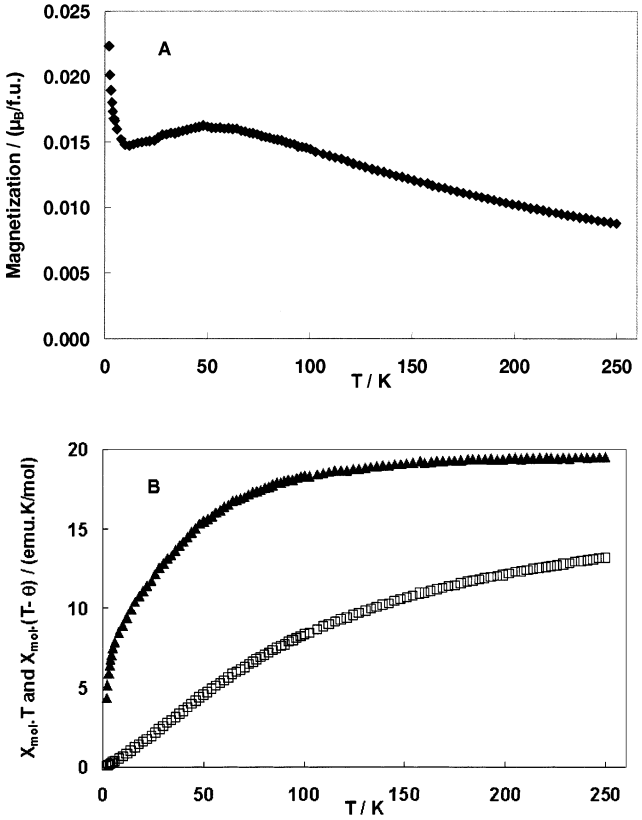

Figure 2. (A) Plot of magnetization versus T. (B) Plot of the $\chi_M \cdot (T)$ (□) and $\chi_M \cdot (T - \theta)$ (△) versus T (with $\theta = -120$ K). The data were recorded in a 0.1 T field, and a correction was made for a small Fe(III) paramagnetic impurity (ca. 1% of the total Fe(III)).

diffraction studies). The second procedure differed from the original synthesis in three ways. First, $Fe(NO_3)_3$ was used instead of $FeCl_3$. Second, deionized water was used instead of 2 M NaCl. Third, the solution containing the α-Na_{12}-$[As_2W_{15}O_{56}]$ and $Fe(NO_3)_3$ was heated at a lower temperature (60 °C versus 80 °C for the original procedure) and for a longer amount of time (1 h versus 5 min for the original procedure).

The IR spectrum of Na**1** was compared with the trivacant starting material α-$Na_{12}[As_2W_{15}O_{56}]$ (see Supporting Information). The spectra of the two compounds are quite similar, including a strong peak at 937 cm^{-1}, corresponding to a terminal W═O stretch.[66] The main difference concerns the asymmetric stretching vibration $W-O_{corner}-W$ which shows two bands in Na**1** and three in α-$Na_{12}[As_2W_{15}O_{56}]$. The electronic spectrum of **1** shows an intense charge-transfer band (oxygen-to-tungsten), which is characteristic of all POMs, along with two shoulder peaks relatively close in energy at 316 and 272 nm.

Magnetic Studies. The temperature dependence of the magnetization of Na**1** was studied in a 0.1 T field (Figure 2). The mean value of the magnetization is weak, suggesting antiferromagnetic coupling of the tetranuclear $[Fe^{III}_4O_{14}(H_2O)_2]$ central unit. A rapid decrease in the susceptibility is observed between 2 and 10 K (Figure 2A). This is attributed to the presence of a small amount of free Fe(III) ions (ca. 1% of the total iron). This paramagnetic contribution, following a Curie law, was subtracted to obtain the actual magnetization of the complex. Coronado and co-workers observed a similar paramagnetic contribution in their studies of αββα-$(Mn^{II}OH_2)_2Mn^{II}_2(P_2W_{15}O_{56})_2^{16-}$ and αββα-$(Ni^{II}OH_2)_2Ni^{II}_2(P_2W_{15}O_{56})_2^{16-}$.[50] They attribute this to the partial decomposition of the sandwich-type compound to give mono- and trisubstituted Wells−Dawson monomers. The product of the magnetic susceptibility plot times the temperature ($\chi_M T$) versus the temperature for Na**1**, corrected for the diamagnetic contributions, is given in Figure 2B. It is interesting to note that the product $\chi_M T$ does not reach a constant value at high temperature. A linear extrapolation up to 300 K gives a value of 14.4 emu·K·mol^{-1}, corresponding to an effective moment of 10.7 μ_B for Na**1**. Hill and co-workers reported a similar value for the phosphorus analogue Na**2** at 10.3 μ_B.[52]

To confirm the antiferromagnetic coupling of the Fe atoms, we sought to obtain a constant value for the product $\chi_M \cdot (T - \theta)$ at high temperature, where θ should be the Curie−Weiss temperature of the $[Fe^{III}_4O_{14}(H_2O)_2]$ unit. This led to a value of −120 K for θ. The corresponding high temperature value of $\chi_M \cdot (T - \theta)$ is 19.5 emu·K·mol^{-1} (Figure 2B). This value is a little higher than that (17.5 emu·K·mol^{-1}) expected for four noninteracting Fe(III) ions. This suggests that the actual absolute value of θ is lower than our estimation, and therefore, the asymptotic behavior of $\chi_M \cdot (T - \theta)$ is only reached at higher temperatures. The antiferromagnetic coupling observed in Na**1** is similar to that reported for αββα-$(Mn^{II}OH_2)_2Mn^{II}_2(P_2W_{15}O_{56})_2^{16-}$, containing isoelectronic Mn(II) ions.[50] However, the intensity of the antiferromagnetic exchange interaction appears to be stronger in Na**1**.

Crystallographic Studies. The X-ray crystal structure of Na**1** consists of a tetranuclear iron core, $[Fe^{III}_4O_{14}(H_2O)_2]$, sandwiched between two trivacant Wells−Dawson α-$As_2W_{15}O_{56}$ 12-moieties (Figure 1). The central M_4 unit is similar to those seen in the phosphorus analogues of formula $[(MOH_2)_2M_2(P_2W_{15}O_{56})_2^{n-}]$, where M = Cu(II),[48] Zn(II),[51] Mn(II),[50] or Fe(III).[52] All of these structures, including Na**1**, display the conventional inter-POM-unit-connectivity known as β in Baker−Figgis notation (β-junctions).[57,58,60,67,68] A comparison of selected bond lengths and angles in Na**1** and the analogous phosphorus complex Na**2** are given in Table 2. As expected, the As−O bond lengths are slightly longer than the analogous P−O bond lengths. However, this has caused little or no structural perturbation of the tungsten−oxygen framework or the central $[Fe^{III}_4O_{14}(H_2O)_2]$ unit, based on the similarity of the bond lengths and angles obtained from these two structures. Bond valence sum (BVS) calculations from the X-ray structure of Na**1** yields average oxidation states of 3.01 ± 0.07 and 2.93 ± 0.07, respectively, for the two Fe sites (Fe1 and Fe2).[69] The usual disorder of cations and solvent molecules makes it impossible to account for their total numbers by X-ray crystallography alone. As a

(66) Rocchiccioli-Deltcheff, C.; Thouvenot, R. *J. Chem. Res., Synop.* **1977**, *2*, 46−47.
(67) Baker, L. C. W.; Figgis, J. S. *J. Am. Chem. Soc.* **1970**, *92*, 3794−3797.
(68) Anderson, T. M.; Hill, C. L. *Inorg. Chem.* **2002**, *41*, 4252−4258.
(69) Brown, I. D.; Altermatt, D. *Acta Crystallogr.* **1985**, *B41*, 244−247.

Table 2. Selected Bond Lengths (Å) and Bond Angles (deg) for Na**1** and Na**2**[52,a]

	Na**1**	Na**2**
W−O_t	1.720(6)	1.701(22)
W−O_b	1.922(7)	1.896(20)
W−O_c	2.320(8)	2.363(20)
W−O_d	2.330(8)	2.373(20)
X−O_c	1.670(6)	1.513(20)
X−O_d	1.716(6)	1.610(20)
X−$O_{d'}$	1.738(6)	1.620(20)
Fe1···Fe2	3.192(7)	3.173(20)
Fe1···Fe1A	3.406(8)	3.381(20)
Fe1···Fe2A	3.177(8)	3.173(20)
Fe2···Fe2A	5.381(8)	5.374(20)
Fe2−OW1	2.004(7)	2.050(20)
O_t−W−O_b (cap)	103.0(3)	104.4(11)
O_t−W−O_b (belt)	99.2(3)	99.5(10)
O_t−W−O_d (cap)	170.9(3)	168.2(10)
O_t−W−O_c (belt)	171.0(3)	172.0(10)
O_d−X−O_c	107.2(3)	107.6(12)
O_d−X−O_c	108.4(3)	107.3(11)
Fe1···Fe2···Fe1A	64.7(3)	64.4(10)
Fe2···Fe1···Fe2A	115.3(3)	115.6(10)

[a] O_t = terminal oxygen; O_b = doubly bridging oxygen; O_c = triply bridging oxygen; O_d = quadruply bridging oxygen; $O_{d'}$ = quadruply bridging oxygen that bonds to the Fe atoms; X = central heteroatom (As(V) in Na**1** and P(V) in Na**2**).

result, elemental analysis and thermogravimetric analysis were used to determine the total number of Na^+ cations and water molecules, respectively.

Electrochemical Studies. To our knowledge, this is the first report on the electrochemical behavior of Na**1** in solution. Recently, the electrochemistry of **1**, entrapped in multilayers of polymers on a glassy carbon electrode, was described, without any indication of a study in solution.[70] Figure 3A gives the cyclic voltammogram of Na**1** in solution superimposed with the trivacant starting material, α-$As_2W_{15}O_{56}^{12-}$.[33] The trivacant α-$As_2W_{15}O_{56}^{12-}$ species is unstable in solution. However, the pH = 5 (0.4 M CH_3COOLi + CH_3COOH) buffer solution renders this lacunary species sufficiently stable over the time scale of a CV study. Between +0.2 and −0.5 V (vs SCE), new waves appear in the CV of Na**1** which were not present in α-$As_2W_{15}O_{56}^{12-}$ (Figure 3A). These waves are assigned to the reduction of the Fe(III) centers, followed by their reoxidation. The Fe(III) centers are known to be more easily reduced than W(VI) centers among a variety of transition-metal-substituted polyoxometalates (TMSPs).[19,30] The typical characteristics of the Fe(III) waves are more prominent when the potential domain is explored only up to the beginning of the first W(VI) wave (Figure 3B). The stepwise reduction of the Fe(III) centers observed in Na**1** was first reported for the phosphorus analogue Na**2**.[52] This phenomenon is probably due to the interactions among the adjacent Fe(III) centers. Analogous observations were also reported for sandwich-type complexes with Keggin moieties, and the authors concluded that electronic interactions involving the metals of the central unit can generate or reinforce inequivalence among the Fe(III) centers.[61a] Controlled potential coulometry confirms that each of the four Fe(III) waves observed in Figure 3B involves a one-electron process.

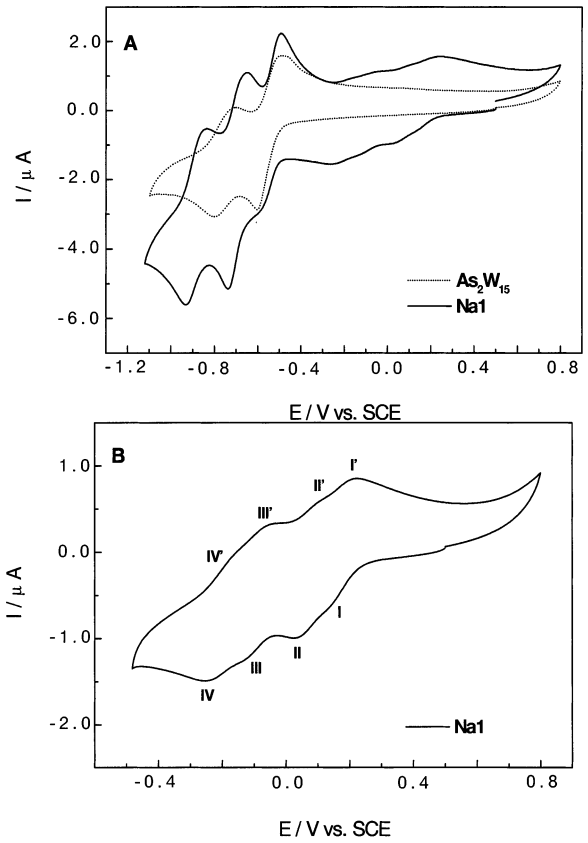

Figure 3. Cyclic voltammograms of α-$As_2W_{15}O_{56}^{12-}$ and Na**1** (2×10^{-4} M) in a pH = 5 buffer solution. The scan rate was 10 mV s^{-1}, the working electrode was glassy carbon, and the reference electrode was SCE. For more detailed information, see the Experimental Section. (A) Superposition of α-$As_2W_{15}O_{56}^{12-}$ (···) and Na**1** (—). (B) Cyclic voltammogram of Na**1** with the reduction potential domain restricted to that of the Fe(III) centers.

Other differences in the CVs of Na**1** and α-$As_2W_{15}O_{56}^{12-}$ are attributable to their respective W(VI) waves, located between −0.5 and −1.120 V (vs SCE). The CV of α-$As_2W_{15}O_{56}^{12-}$ is composed of a two-wave system: the first wave features a four-electron process ($E_{pc1}{}^W = -0.600$ V; $E_{pa1}{}^W = -0.500$ V) which is followed by a second wave representing a two-electron process ($E_{pc2}{}^W = -0.792$ V; $E_{pa1}{}^W = -0.712$V). For Na**1**, a three-wave system replaces the two-wave pattern observed in α-$As_2W_{15}O_{56}^{12-}$ over this potential domain ($E_{pc1}{}^W = -0.590$ V; $E_{pa1}{}^W = -0.494$ V; $E_{pc2}{}^W = -0.736$ V; $E_{pa2}{}^W = -0.656$ V; $E_{pc3}{}^W = -0.930$ V; $E_{pa3}{}^W = -0.838$ V). The first wave of Na**1** is located at approximately the same potential as the first wave of α-$As_2W_{15}O_{56}^{12-}$, but the shape of the latter is distinctly different from that of the former. The observed modifications in the CV patterns of Na**1** and α-$As_2W_{15}O_{56}^{12-}$ are most likely due to subsequent changes in the acid−base properties of POMs upon reduction. However, it must be pointed out that the number of W waves observed for Na**1**, and hence the electron number for each wave, depends on the pH of the electrolyte. When the potential of the working electrode is driven beyond the location of the third W(VI) wave in Na**1**, the reoxidation pattern features

(70) Bi, L. H.; Liu, J. Y.; Shen, Y.; Wang, E. K.; Dong, S. J. *Gaodeng Xuexiao Huaxue Xuebao* **2002**, *23*, 472−474.

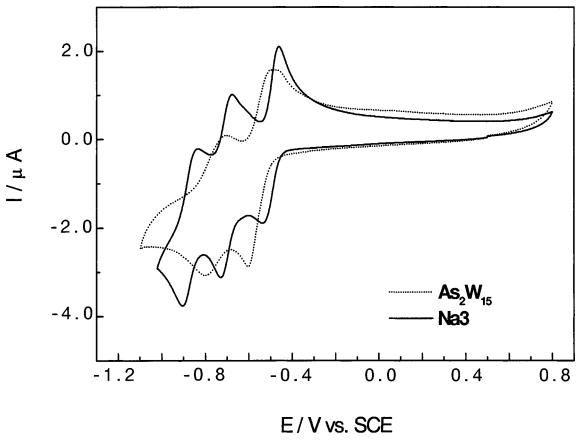

Figure 4. Cyclic voltammograms of α-$As_2W_{15}O_{56}^{12-}$ and Na**3** (2×10^{-4} M) in a pH = 5 buffer solution. The scan rate was 10 mV s^{-1}, the working electrode was glassy carbon, and the reference electrode was SCE. For more detailed information, see the Experimental Section.

the characteristics of a deposit on the electrode surface. This observation is in agreement with those obtained with various other TMSPs when more than six electrons are added to each complex.[21,52] These electrode modifications are beyond the scope of this manuscript, where the electrochemical studies are restricted only to the reversible diffusion waves.

Role of the Metals in the Central M_4 Unit. The observation that the two-wave system observed in α-$As_2W_{15}O_{56}^{12-}$ is replaced by a three-wave system in Na**1** prompted us to investigate whether this behavior is a consequence of the types of metals in the M_4 central unit or whether it was a common feature of all the sandwich-type POMs derived from α-$As_2W_{15}O_{56}^{12-}$. An electrochemical study of the known complex, $\alpha\beta\beta\alpha$-$Na_{16}(Zn^{II}OH_2)_2Zn^{II}_2(As_2W_{15}O_{56})_2$ (Na**3**), proved to be particularly useful in resolving this issue.[55a] Figure 4 shows the superposition of the CVs of Na**3** and α-$As_2W_{15}O_{56}^{12-}$ in a pH = 5 buffer solution. As expected, the electroactivity of Na**3** is confined to the same potential domain as that of α-$As_2W_{15}O_{56}^{12-}$. Like Na**1**, a new three-wave pattern is observed for Na**3** in place of the two-wave pattern characteristic of α-$As_2W_{15}O_{56}^{12-}$. A comparison of the CVs of Na**1** and Na**3** (Figures 3A and 4, respectively), however, indicates that the first two tungsten waves of the latter complex (Na**3**) are better separated than the corresponding ones in Na**1**. This observation again underscores the significance of the nature of the metals of the central M_4 unit modulating the acid−base properties of the reduced forms of the complexes. It is worth noting that all of the curves in Figures 3 and 4 are well defined in the pH = 5 medium. In general, well-behaved waves were observed for these complexes between pH = 3 and pH = 6. These reports are in sharp contrast with those of Ruhlmann and co-workers on the analogous phosphorus complex Na**2**.[59a] They found that when pH > 4, the CV of Na**2** becomes ill-defined with much smaller peak currents.

Electrocatalytic Reduction of O_2 and H_2O_2. One incentive to study Na**1** and its analogues is their potential application in electrocatalytic reduction reactions. Dioxygen

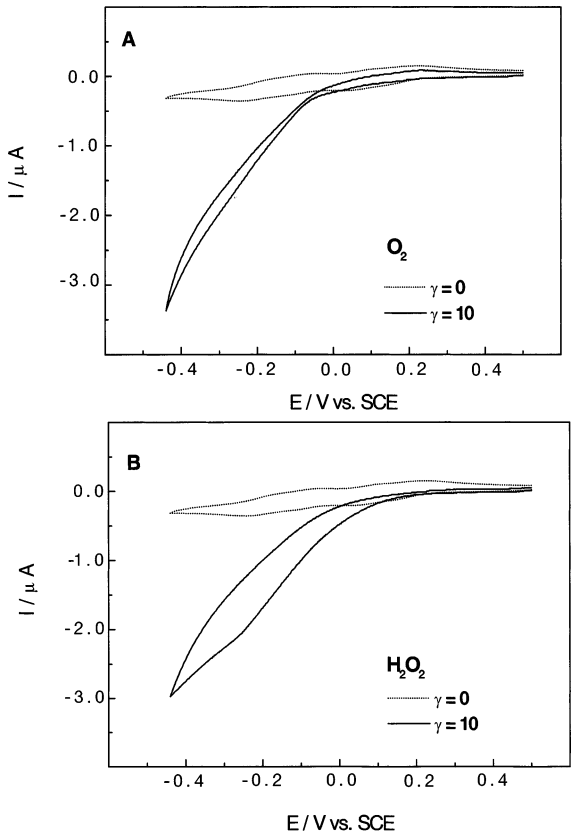

Figure 5. Superposition of the cyclic voltammograms obtained in the presence of 1×10^{-4} M Na**1** in a pH = 5 buffer solution in the absence or presence of (A) O_2 or (B) H_2O_2. The scan rate was 2 mV s^{-1}, the working electrode was glassy carbon, and the reference electrode was SCE. The excess parameter γ is defined as $C°$ (O_2)/$C°$ (POM) for dioxygen and $C°$ (H_2O_2)/$C°$ (POM) for hydrogen peroxide, respectively.

was selected as the first candidate in the present work because it is abundant and environmentally benign, yet very challenging to use as a selective oxidant.[71] Hydrogen peroxide was also selected as a substrate because it may be useful in assessing the nature of the final product in the electrocatalytic reduction of dioxygen. It is also an important oxidant in its own right. The main features of the electrocatalytic reduction of O_2 and H_2O_2 (in pH = 5 buffer solution) are shown in Figure 5. The direct electroreductions of O_2 and H_2O_2 (in the absence of any catalyst) are only observed at fairly negative potentials.[72] In contrast, Figure 5A shows that in the presence of Na**1** the electrocatalytic reduction of O_2 proceeds readily at +0.015 V. Interestingly, this reaction occurs over the potential domain that we previously established corresponds to the reduction of the Fe(III) centers. This suggests that the Fe(III) centers play a very important role in the reaction. Figure 5B shows that the electrocatalytic reduction of H_2O_2 proceeds at +0.100 V, just past the first Fe(III) reduction center. This result is consistent with the fact that the electrocatalytic reduction of H_2O_2 (in the presence of Na**1**) is more facile than that of O_2. This pattern suggests that the final product in the reduction of O_2 under these conditions is water.

(71) Hill, C. L.; Weinstock, I. A. *Nature* **1997**, *388*, 332−333.
(72) Keita, B.; Benaïssa, M.; Nadjo, L.; Contant, R. *Electrochem. Commun.* **2002**, *4*, 663−668.

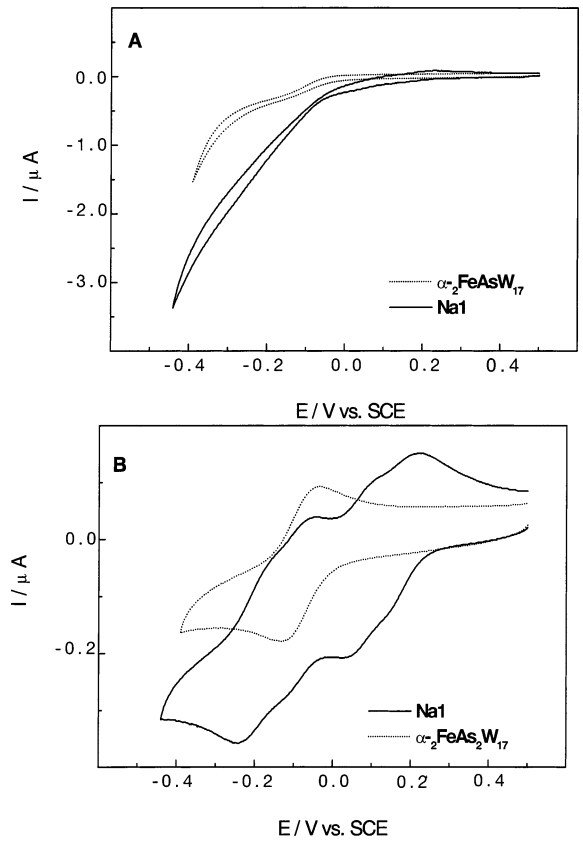

Figure 6. (A) Comparison of the electrocatalytic reduction of dioxygen ($\gamma = 10$) by 1×10^{-4} M Na**1** (—) and α_2-$As_2(Fe^{III}OH_2)W_{17}O_{61}^{7-}$ (···) in a pH = 5 buffer solution. The scan rate was 2 mV s^{-1}, the working electrode was glassy carbon, and the reference electrode was SCE. (B) Same as (A) except that the reduction potential domain is restricted to that of the Fe(III) centers.

Finally, it is interesting to compare the differences in the activity of Na**1** with those of the recently studied monosubstituted complex α_2-$As_2(Fe^{III}OH_2)W_{17}O_{61}^{7-}$.[35] Figure 6A shows a remarkable positive potential shift in the electrocatalytic reduction of O_2 by Na**1** compared to that of α_2-$As_2(Fe^{III}OH_2)W_{17}O_{61}^{7-}$. Figure 6B, restricted to the reduction of the Fe(III) centers, compares the behavior of Na**1** and α_2-$As_2(Fe^{III}OH_2)W_{17}O_{61}^{7-}$ in the strict absence of dioxygen. The Fe(III) redox process of the monosubstituted complex (α_2-$As_2(Fe^{III}OH_2)W_{17}O_{61}^{7-}$) occurs at a more negative potential in a pure argon atmosphere than that observed for the first two Fe(III) waves of Na**1**. This led us to conclude that Na**1** is a better catalyst than α_2-$As_2(Fe^{III}OH_2)W_{17}O_{61}^{7-}$ for the reduction of O_2. These results again suggest that the enhanced catalytic effect observed for Na**1** may be due to cooperativity effects among the Fe(III) centers in the central M_4 unit of Na**1**.

Acknowledgment. This work was supported in part by the University Paris XI and the CNRS (UMR 8000 and 8648). We also thank NSF Grant CHE-9975453 for the research, Grant CHE-9974864 for funding the D8 X-ray instrument, and Wade Neiwert for assistance with X-ray crystallography.

Supporting Information Available: Structure determination parameters, crystal and structure refinement data, atomic coordinates and isotropic displacement coefficients, bond lengths and angles, anisotropic displacement parameters, infrared, and magnetization data for Na**1**. This material is available free of charge via the Internet at http://pubs.acs.org.

IC0261169